JOURNAL OF GEOPHYSICAL RESEARCH, VOL. 104, NO. A10, PAGES 22,375–22,388, OCTOBER 1, 1999

A synthesis of solar cycle prediction techniques

David H. Hathaway, Robert M. Wilson, and Edwin J. Reichmann
NASA Marshall Space Flight Center, Huntsville, Alabama

Abstract. A number of techniques currently in use for predicting solar activity on a solar cycle timescale are tested with historical data. Some techniques, e.g., regression and curve fitting, work well as solar activity approaches maximum and provide a month-by-month description of future activity, while others, e.g., geomagnetic precursors, work well near solar minimum but only provide an estimate of the amplitude of the cycle. A synthesis of different techniques is shown to provide a more accurate and useful forecast of solar cycle activity levels. A combination of two uncorrelated geomagnetic precursor techniques provides a more accurate prediction for the amplitude of a solar activity cycle at a time well before activity minimum. This combined precursor method gives a smoothed sunspot number maximum of 154 ± 21 at the 95% level of confidence for the next cycle maximum. A mathematical function dependent on the time of cycle initiation and the cycle amplitude is used to describe the level of solar activity month by month for the next cycle. As the time of cycle maximum approaches a better estimate of the cycle activity is obtained by including the fit between previous activity levels and this function. This Combined Solar Cycle Activity Forecast gives, as of January 1999, a smoothed sunspot maximum of 146 ± 20 at the 95% level of confidence for the next cycle maximum.

1. Introduction

Accurate predictions of the levels of solar activity are increasingly important as we become more reliant upon satellites in low-Earth orbits. Such satellites often provide crucial links in communications and national defense and are also often the source of important scientific information. Their orbits, however, may place them in jeopardy at times of high solar activity. The increased ultraviolet emission from the Sun at such times heats the Earth's upper atmosphere causing it to expand and increase the drag on these satellites, thereby leading to early reentry into the Earth's atmosphere. Long-term predictions of solar activity are therefore essential to help plan missions and to design satellites that will survive for their useful lifetimes.

Ideally, we would like to predict solar activity using a model of the Sun's magnetic dynamo along with observations of current and past conditions to initialize that model. Unfortunately, both the model and many of the important observations do not exist at present. We recognize that solar magnetism is the key to understanding the processes involved. We believe that the Sun's differential rotation, meridional circulation, and large-scale convective motions all play important roles in producing the cyclic magnetic behavior that we observe. We have not yet, however, produced a theory that fully incorporates these mechanisms in a model that provides any predictive power.

Given this state of the art, we are forced to predict solar activity by statistical methods that rely on determining correlations between past and future behavior. It is not surprising that these attempts at solar cycle prediction are often looked upon as something less than scientific and only slightly better than "astrology." This has become painfully clear in our survey of the various prediction techniques. Many fine papers on this topic have only appeared as technical notes, memos, reports to granting institutions, or papers in conference proceedings (apparently unable to pass muster in the refereed literature).

Here we will show that we can make more reliable predictions of solar cycle activity by combining different prediction methods. A fairly extensive, and well representative, series of techniques are examined in sufficient detail to reproduce those techniques for testing with historical data. Some techniques were discarded simply because they provided too little predictive power. Others were examined and found promising but were not considered due to our inability to test the techniques over the last four cycles. In the process of examining these techniques we found several interesting results that may, in fact, point toward new physical processes that contribute to producing the Sun's 11-year activity cycle.

Paper number 1999JA900313.

In this study, our goal is to synthesize a prediction technique that will provide more reliable estimates of the levels of solar activity several years into the future. In the next section we present the various datasets that best describe the solar activity cycle. One fundamental problem associated with solar cycle predictions is the small number of solar cycles that are well observed. Complete daily sunspot observations go back only to 1849 and geomagnetic observations only to 1868. Therefore most of our efforts at predicting solar cycle activity levels are faced with the statistics of small numbers: 10 to 20 cycles. In section 3 we present a number of prediction techniques based largely on correlations extracted from these data sets. In section 4 we test these techniques by using them to predict the behavior of the last four complete cycles (cycles 19-22 in the Zürich numbering system). Our synthesis of a better prediction method is then given in section 5, and it is followed by our conclusions in the final section.

2. The Data

2.1. Solar Activity Indicators

Sunspot numbers provide perhaps the most useful data for solar cycle predictions. While sunspot observations extend back to the time of Galileo, regular observations of use in characterizing the solar cycle did not begin until about 1750. The relative sunspot number R is derived from a formula due to *Wolf* [1852] that is heavily weighted by the number of sunspot groups observed:

$$R = k(10g + n), \tag{1}$$

where g is the number of spot groups, n is the number of individual spots, and k is a factor that accounts for observer, telescope, and observing conditions. This formula has the advantage of being relatively insensitive to the uncertainties in identifying small individual spots. The International Sunspot Number (formerly known as the Zürich or Wolf Number) is now compiled and reported by the Sunspot Index Data Center in Brussels, Belgium and is the one recognized as the standard. Additionally, there is the Boulder Sunspot Number, compiled and reported by the U.S. National Oceanic and Atmospheric Administration (NOAA) Space Environment Center in Boulder, Colorado, and the American Number, compiled by the American Association of Variable Star Observers. Generally speaking, the timing and amplitudes of these measures agree remarkably well, although the International Number tends to be the more conservative estimate. Monthly averages of the International Sunspot Number are shown in Figure 1 for the years 1750 through 1998. Figure 1 shows both the cyclic behavior and variations in amplitude, shape, and duration from cycle to cycle. It is these variations, of course, that make predictions difficult.

Geomagnetic indices constitute another source of useful datasets indicating solar activity levels. Solar flares, prominence eruptions, and coronal mass ejections produce variations in the solar wind that, in turn, cause fluctuations in the Earth's magnetic field. Continuous observations of these fluctuations extend back to 1868. Several different indices are used to quantify the level of geomagnetic activity, [cf. *Mayaud,* 1980]. The K indices give the amplitude of the irregular variations over 3-hour intervals on a quasi-logarithmic scale. The Kp index is a "planetary" K index derived from observations taken globally by a network of stations and reported for 3-hour intervals since 1932. The ap index is equivalent to the Kp index but uses a linear scale that makes averaging easier. The two most frequently used indices for solar cycle predictions are the Ap index and the aa index. The Ap index is a daily average of the ap indices and is available from 1932. The aa index is a daily index with a linear scale from two nearly antipodal observing stations (presently Hartland Observatory in the United Kingdom and Canberra Observatory in Australia) and is available from 1868. The monthly

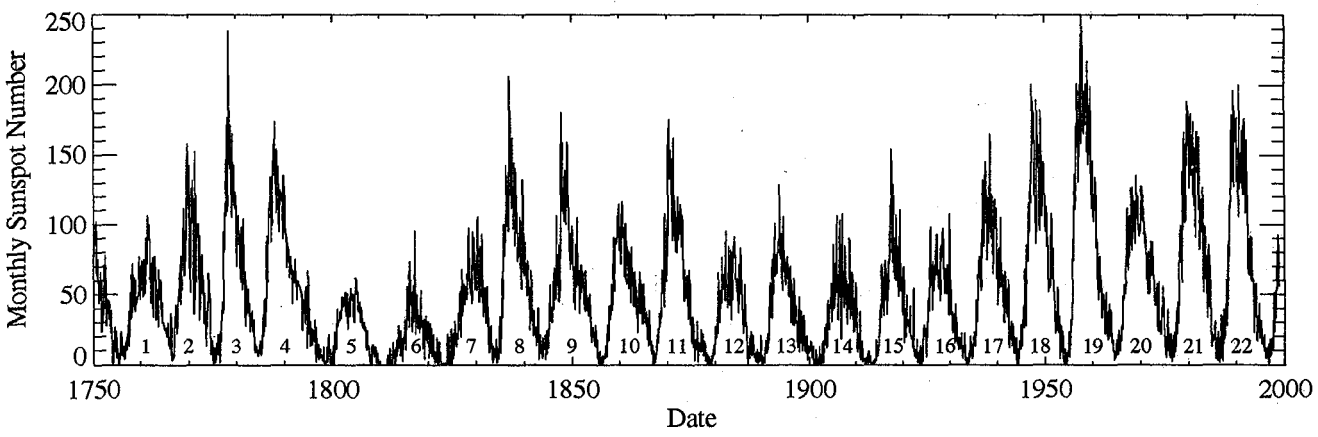

Figure 1. Monthly averaged International Sunspot Number as a function of time. The individual sunspot cycles (numbered along the bottom) vary in amplitude, duration, and shape.

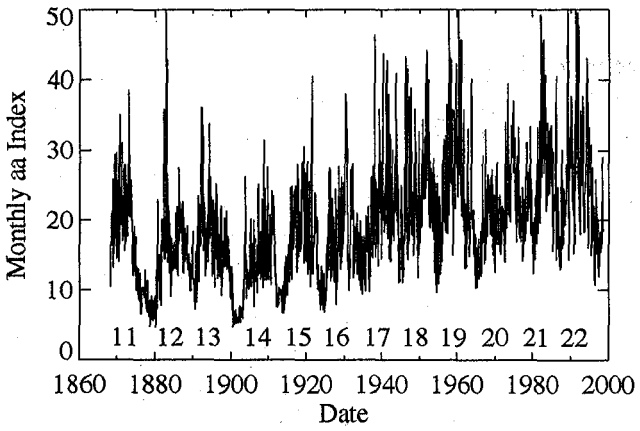

Figure 2. Monthly averaged geomagnetic index *aa* as a function of time. The solar activity cycle is not as obvious here although peaks in geomagnetic activity do tend to coincide with solar activity peaks (identified by the cycle numbers along the bottom).

values of the *aa* index are plotted in Figure 2 for the years 1868 through 1998.

2.2. Data Preparation

All indicators of solar activity are inherently noisy. The solar phenomena that produce the activity are noisy themselves. In addition, these signals are often measured in ways that introduce additional variations. Some signal processing is required to isolate the component associated with the solar activity cycle and its characteristic timescale of 11 years. Most indicators originate as daily values but are averaged monthly to remove variations associated with the Sun's 27-day synodic rotation period. The monthly values require additional averaging to produce a signal without wild oscillations from month to month. A commonly used average is the "12-month moving average" or "13-month running mean" as it is now more commonly referred to. If R_n is the monthly averaged sunspot number for month n, then the 13-month running mean is given by

$$\bar{R}_n = \frac{1}{24}\sum_{i=-6}^{5} R_{n+i} + \frac{1}{24}\sum_{i=-5}^{6} R_{n+i}. \qquad (2)$$

This filtering smoothes out most variations with periods less than a year and it is centered on month n. Although it is widely used (references to "smoothed" sunspot numbers usually indicate the use of this filter), it is not the best filter for isolating solar cycle timescales. The monthly values that it uses are themselves averages of different length and the triangular tapering at both ends of the 13-month average still allows some high-frequency signals to pass. Gaussian-shaped filters with widths of a year or more are more suitable for studies of solar cycle characteristics. A Gaussian-shaped filter has the important property of having a Gaussian-shaped frequency response. It attenuates high-frequency components with monotonically increasing efficiency as the frequency increases. One example of such a filter is given with relative weights

$$W(t) = e^{-0.3t^2/a^2} - e^{-1.2}\left(2.2 - 0.3t^2/a^2\right), \qquad (3)$$

where t is the time difference from the center of the filter and a is a parameter that gives the width of the filter. The full-width at half-maximum (FWHM) is $2a$, and the filter weight and its first derivative both vanish at $t = \pm 2a$.

Smoothed sunspot numbers are plotted in Figure 3 using both the 13-month running mean and the Gaussian-shaped filter with a FWHM of 24 months. The 13-month filter leaves variations with periods considerably less than 1 year while the 24-month filter effectively removes these high-frequency components. The disadvantage with the 24-month filter is that it requires data 23 months on either side of its central point. Another disadvantage of the 24-month Gaussian filter is its inability to follow the rapid change in slope at the start of the cycles. While an 18-month Gaussian does better in following this bend it also passes shorter-period variations. We prefer the 24-month Gaussian for determining solar cycle statistics such as maximum, minimum, and period. The commonly used 13-month running mean can be both ambiguous (by providing multiple extrema) and misleading in determining these solar cycle statistics.

3. Prediction Techniques

Numerous techniques have been devised to predict solar cycle activity levels. In particular, *Vitinskii* [1965] discusses several techniques that were available at the time of his writing, 1962. Here we divide the techniques

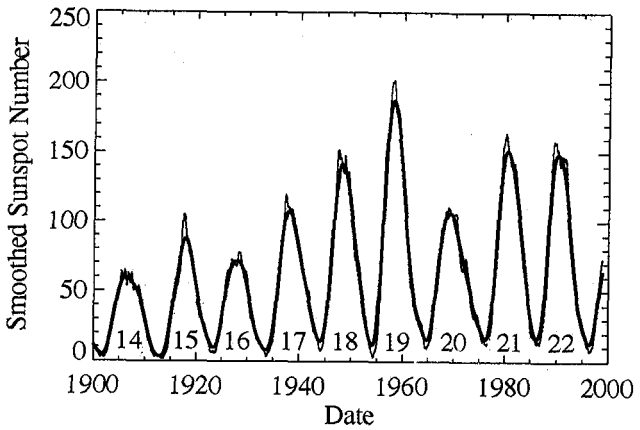

Figure 3. Smoothed sunspot numbers. The thin line gives the monthly sunspot numbers smoothed with the standard 13-month running mean. The thick line gives the monthly sunspot numbers smoothed with a Gaussian-shaped filter having a FWHM of 24 months. The 13-month running mean retains variations with time-scales as short as 6 months. The wider, Gaussian, filter removes these high-frequency oscillations and gives lower maxima and higher minima.

into two categories: regression techniques and precursor techniques. The regression techniques use observed values of solar activity from the recent past to extrapolate into the near future. These techniques include standard regression and autoregression, curve-fitting, and neural networks. They usually provide forecasts of future activity levels as a function of time at monthly or yearly intervals and often extend for a complete solar cycle or more into the future. The precursor techniques provide an estimate of the amplitude for the next solar cycle. As the name implies, precursor techniques provide such estimates well before the sunspot cycle has "officially" started.

3.1. Regression Techniques

A variety of models are used to describe the behavior of a sunspot cycle. They can be separated into two categories using the form of the model: an average cycle shape or a mathematical function that mimics that shape. An average sunspot cycle shape is used explicitly in the methods based on the work of *McNish and Lincoln* [1949], while implicit average cycle shape models are used in neural network techniques [*Calvo et al.*, 1995; *Conway et al.*, 1998]. Mathematical functions for the shape of the cycle have been proposed by *Stewart and Panofsky* [1938], *Elling and Schwentek* [1992], and *Hathaway et al.* [1994].

McNish and Lincoln [1949] proposed a regression technique for predicting solar activity levels one year into the future. They used an average sunspot cycle constructed from smoothed sunspot numbers starting with cycle 8 in February 1834. They found that the sunspot numbers from the earlier cycles (1-7) are statistically different and thus chose to exclude them from the average. First, the monthly averaged sunspot numbers are smoothed with the 13-month running mean. Next, the average cycle is constructed by sampling this running mean at 12-month intervals starting at the month of minimum for each cycle and averaging the results for cycles 8 through the last complete cycle at years 0 through 11. Deviations from the average for each cycle are then used to find regression coefficients that predict the smoothed sunspot number for the next year. They concluded that the most useful regression only uses the deviation from the mean for the current year. Thus, for year $n+1$ into the cycle the predicted sunspot number will be

$$R'_{n+1} = \bar{R}_{n+1} + k_n \Delta R_n, \qquad (4)$$

where $\bar{R}_{n+1}$ is the smoothed sunspot number for year $n+1$ averaged over the previous cycles starting with cycle 8, k_n is the regression coefficient for year n, and ΔR_n is the deviation from the average smoothed sunspot number for the current year. The regression coefficients are determined by minimizing the sum of the RMS differences between the predicted and observed variations from the mean cycle at year n. This minimization gives

$$k_n = \sum_{m=8}^{M} \Delta R_{n,m} \Delta R_{n+1,m} / \sum_{m=8}^{M} \Delta R_{n,m}^2, \qquad (5)$$

where the index m identifies the sunspot cycle number and M is the last complete cycle. Certain drawbacks with this technique exist however, including the fact that it provides predictions only one year in advance and that the temporal sampling is at yearly intervals.

Several modifications have been employed to make the McNish-Lincoln method more accurate and useful. For example, the technique can be used recursively to give predictions for a complete solar cycle by using the predicted value to project the prediction year by year into the future. Another modification has been to shorten the sampling interval to single months. While the technique has been improved, a basic problem remains; namely, relying on the average cycle to serve as the base prediction. The average cycle does not adequately account for systematic changes in cycle shape. For example, *Waldmeier* [1935, 1939] has noted that large-amplitude cycles tend to take less time to reach their maxima than do small-amplitude cycles. This "Waldmeier effect" produces systematic errors in predicting both the timing of maximum and the level of solar activity during the declining phase of a solar cycle. Efforts to remedy this problem include using an average aligned at minimum for the rising phase and a second average aligned at maximum for the declining phase [*Greer*, 1993; *Niehuss et al.*, 1996].

We examined two variations on the technique of McNish and Lincoln. The first is a Modified McNish-Lincoln method that uses data from cycle 9 onward to calculate the mean cycle and the regression coefficients. It is used recursively to predict monthly values for the remainder of a cycle using equation (5) to evaluate the regression coefficients at monthly intervals. This is a method previously used by the Space Environment Services Center in Boulder, Colorado. The second method, the Marshall Solar Activity Future Estimation (MSAFE) method, has been described by *Niehuss et al.* [1996] and is currently used by the Space Environment and Effects Program at NASA's Marshall Space Flight Center. This method uses the technique of *Holland and Vaughan* [1984] to calculate mean cycles using data from cycle 1 to the present. Holland and Vaughn suggest using a Lagrangian technique which stretches and contracts each cycle to the average cycle length before averaging the results. During the rising phase of solar activity the MSAFE method uses a mean cycle that extends from minimum to minimum. For the declining phase of the cycle it uses an average cycle that extends from maximum to maximum. The cycle prediction method is a recursive McNish-Lincoln method that uses monthly deviations from the mean cycle to calculate the regression coefficients that predict the next month's value throughout the cycle.

The problem of systematic variations in cycle shape that are unaccounted for by the mean cycle shape is easily addressed using parametric equations for a determination of the shape of the solar activity cycle. *Stewart and Panofsky* [1938] proposed a function for the shape of the cycle with the form

$$R(t) = a(t - t_0)^b e^{-c(t-t_0)}, \quad (6)$$

where a, b, c, and t_0 are parameters that vary from cycle to cycle. This gives a power law for the rising phase of the cycle and an exponential for the declining phase. They used several methods to determine these parameters for cycles 1-16 employing cycle statistics such as time of minimum, time of maximum, size of maximum, and integrated sunspot number. They found a substantial scatter in the results from the various methods, finding that some cycles could not be fit using some statistic combinations and that some cycles were poorly fit, at best. However, some of this scatter might be attributed to their methods of fitting the function to the data, since these methods were limited by the computational resources of that era. They concluded, nonetheless, that such functions could provide a good description of the level of solar activity over a solar cycle. They also noted that the parameters appeared to depend upon each other in a way which indicated that fewer parameters might be required.

Elling and Schwentek [1992] offered another fit using a modified F-distribution density function requiring five parameters. Although this may seem like a step in the wrong direction, their results showed that some parameters did not vary while others varied in unison. More importantly, they found that reliable forecasts could be made for the remainder of a cycle after $\tilde{3}$ years had elapsed from the time of minimum.

More recently, *Hathaway et al.* [1994] found a similarly shaped function that only requires two parameters for each solar cycle: a starting time t_0 and an amplitude a with

$$R(t) = a(t - t_0)^3 / [e^{(t-t_0)^2/b^2} - 0.71]. \quad (7)$$

The dependent parameter b is given by

$$b(a) = 27.12 + 25.15/(a \times 1000)^{1/4} \quad (8)$$

and is directly related to the number of months between minimum and maximum (time is measured in units of months for equations (7) and (8)). This dependence of b upon the amplitude a is indicative of the Waldmeier effect. It produces cycles with different shapes depending upon their amplitudes. Hathaway et al. found that this simple function of two parameters fits the behavior of cycles 10-21 as well or better than the five-parameter function of *Elling and Schwentek* [1992]. They too, found that the fit to a cycle was well determined within $\tilde{3}$ years of minimum.

A common drawback to these regression techniques is the length of time required to find a good estimate for the behavior of a solar cycle. It usually takes about 3 years from minimum before the cycle is well characterized. Alternate techniques are obviously needed to characterize a cycle near, or even before, sunspot minimum.

3.2. Precursor Techniques

A number of features of the solar activity cycle provide advance information on the amplitude of the cycle. Some of these features are found in the record of sunspot numbers and some in the geomagnetic indices. While we classify methods using any of these features as precursor methods, it should be noted that many researchers in this field reserve the precursor classification for the methods that employ only the geomagnetic indicators. Given this distinction, we separate the techniques according to the dataset they employ.

3.2.1. Sunspot number indicators. A number of patterns have been perceived in the sunspot record [*Vitinskii,* 1965; *Wilson et al.,* 1998a]. These patterns are usually surmised from cycle statistics such as cycle maximum, minimum, and period. The original discovery, and subsequent rediscoveries, of these patterns usually used either yearly averages of sunspot numbers or the 13-month running mean. In reexamining these patterns we will use the 24-month Gaussian mean. Table 1 gives the cycle statistics derived from International Sunspot Number smoothed using the 24-month FWHM Gaussian filter. The cycle number is given by n. The sunspot number minimum at the start of the cycle is R_{min} and the month in which this minimum occurred is E_{min}. The cycle maximum is R_{max} and the month in which it occurred is E_{max}. The period of the cycle in months from minimum to minimum is Per.

The average cycle gives the simplest of the precursor prediction techniques and provides a point of comparison for the other prediction techniques. The amplitude of the next cycle is simply taken to be the average of the amplitudes of previous cycles. The form of this average remains a point of controversy nonetheless. Some propose using all available data, cycles 1-22, while others argue for excluding the early cycles and only using cycles 8-22 or 10-22. The Average Cycle Method for cycles 1-22 gives

$$R_{max} = 102.6 \pm 38.0 \quad (9)$$

where the uncertainty represents one standard deviation from the mean.

The next simplest prediction technique is to look for linear secular trends and predict that the next cycle will follow that trend. The Secular Trend Method for cycles 1-22 gives

$$R_{max}(n) = 74.8 + 2.42n \pm 34.6. \quad (10)$$

This provides only a marginal improvement over using the average cycle as judged by the slight decrease in the standard deviation. The relationship between cycle am-

Table 1. Sunspot Cycle Statistics Using Monthly Sunspot Numbers Smoothed With a 24-month FWHM Gaussian Filter

n	R_{min}	E_{min}	R_{max}	E_{max}	Per	n	R_{min}	E_{min}	R_{max}	E_{max}	Per
1	10.7	1755/08	72.3	1761/06	127	13	6.4	1889/06	81.0	1893/09	147
2	18.6	1766/03	99.8	1770/03	113	14	4.7	1901/09	59.5	1906/05	135
3	14.4	1775/08	136.2	1778/09	106	15	3.0	1912/12	87.8	1917/12	125
4	15.5	1784/06	130.1	1788/04	168	16	9.5	1923/05	71.5	1927/12	124
5	5.5	1798/06	45.5	1804/06	147	17	7.7	1933/09	107.9	1937/12	124
6	0.8	1810/09	43.4	1816/08	147	18	14.2	1944/01	141.5	1948/03	121
7	3.4	1822/12	66.9	1829/10	130	19	11.6	1954/02	187.2	1958/03	128
8	12.2	1833/10	128.7	1837/05	119	20	15.5	1964/10	106.5	1969/03	137
9	15.6	1843/09	114.6	1848/06	150	21	16.1	1976/03	151.4	1980/06	120
10	7.3	1856/03	91.6	1860/03	131	22	16.6	1986/03	149.0	1990/03	123
11	12.9	1867/02	120.7	1870/12	139	23	12.7	1996/06			
12	5.8	1878/09	64.3	1883/12	129						

plitude and cycle number gives a rather low correlation coefficient ($r = 0.414$) with a substantial probability ($P = 0.324$) that this may occur purely by chance. The mean cycle and the secular trend are both shown in Figure 4.

The next logical step for using trends in cycle amplitudes is to look for periodicities. Two different cyclic variations in cycle amplitude are widely discussed in the literature. One is the "Gleissberg," or "long-period," cycle with a period of 80 to 90 years [*Gleissberg*, 1942]. The second is the Even-Odd effect, which has a period of two cycles in which the odd-numbered cycles have comparable or larger amplitude than the preceding even-numbered cycles [*Gnevyshev and Ohl*, 1948; *Vitinskii*, 1965, *Wilson*, 1992]. The Gleissberg cycle is most apparent prior to cycle 19. The more recent cycles, however, do not appear to conform to the periodicity as seen in the earlier cycles but instead suggest a longer period variation. On the other hand, the Even-Odd effect is most apparent in the recent cycles, particularly from cycle 10 onward.

The Gleissberg cycle is used as a predictive tool by removing the secular trend and then finding the best fit between the residual amplitudes and a cyclic variation with a period between 77 and 99 years (7 to 9 sunspot cycles). The Gleissberg Cycle Method for cycles 1-22 gives

$$R_{max}(n) = 74.8 + 2.42n + 27.4\sin[2\pi(n-0.0)/8.4] \pm 28.3 \quad (11)$$

This yields a period of about 92 years for the Gleissberg cycle and a slight improvement over using the mean or the secular trend for predicting cycle amplitudes. The correlation between the predicted and observed amplitudes gives $r = 0.670$ and the probability that this correlation is due to chance is small ($P = 0.018$). The Gleissberg cycle variation is shown in Figure 5.

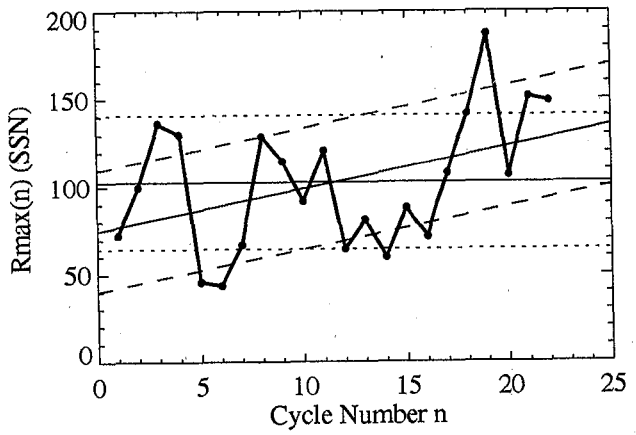

Figure 4. Cycle amplitude versus cycle number. The mean cycle amplitude is represented by the thick horizontal line. The standard deviation about this mean is shown by the dotted lines. The secular trend is shown by the thin line and the standard deviation about this trend is shown with the dashed lines. The secular trend over the 22 cycles provides little improvement over the mean cycle for predicting cycle amplitudes.

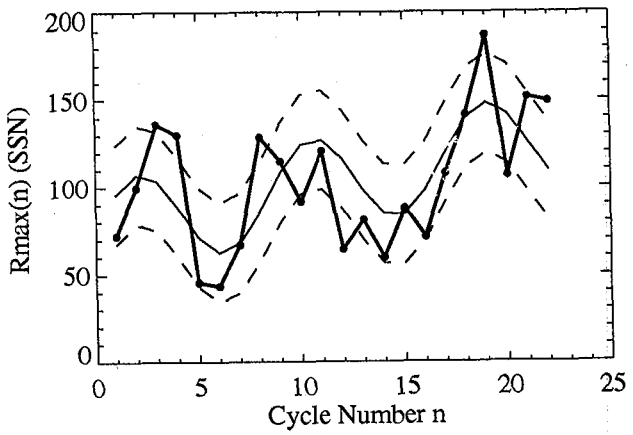

Figure 5. Gleissberg cycle variations in cycle amplitude. The Gleissberg cycle as given by equation (11) is shown with the solid line. The standard deviation about these values is shown with the dashed lines.

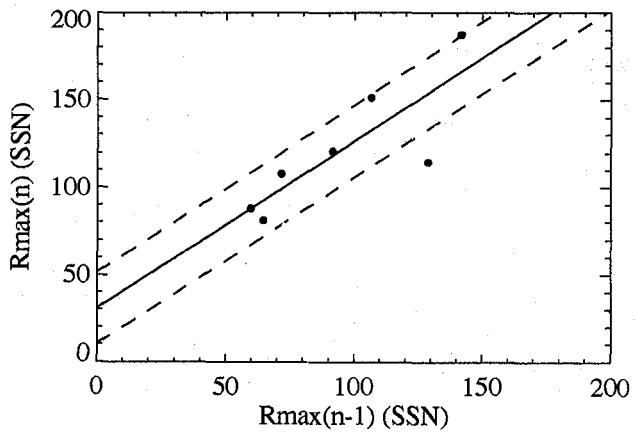

Figure 6. The Even-Odd Method for cycles 8-21. The odd-numbered cycles tend to have maximum amplitudes 30 sunspot numbers higher than the amplitudes of the preceding even-numbered cycles. This relationship is shown with the solid line. The standard deviation about this line is shown with the dashed lines.

The Even-Odd Method is explicitly only useful for predicting the amplitude of odd-numbered cycles. To predict the amplitude of an odd-numbered cycle we must determine the relationship between the amplitudes of the even and odd numbered cycles and apply that relationship to the next odd-numbered cycle. For cycles 1-22, only the cycle pair 4/5 appears to be anomalous. If we only include the cycles with nearly continuous daily observations (cycles 8-21) the Even-Odd Method gives

$$R_{max}(n) = 30.8 + 0.96R_{max}(n-1) \pm 20.6 \qquad (12)$$

with a correlation coefficient $r = 0.831$ and a probability $P = 0.146$ that this correlation is due to chance. We illustrate this method in Figure 6 and note that it gives a significant reduction in the variations as compared to those obtained with the mean cycle.

Two other methods based on sunspot numbers are the Amplitude-Period Method and the Maximum-Minimum Method [*Wilson et al.*, 1998a]. With the Amplitude-Period Method the amplitude of the next cycle maximum is inversely proportional to the period of the previous cycle. For cycles 2-22 the Amplitude-Period Method gives

$$R_{max}(n) = 346.9 - 1.84Per(n-1) \pm 27.8, \qquad (13)$$

where $Per(n-1)$ is the period of the previous cycle in months. This relationship between amplitude and period has a correlation coefficient of $r = -0.687$ with a probability $P = 0.007$ that it is due to chance and it is found to provide a modest reduction in the prediction errors. The Amplitude-Period Method is illustrated in Figure 7.

With the Maximum-Minimum Method the amplitude of the cycle maximum is proportional to its amplitude at minimum. For cycle 1-22 the Maximum-Minimum Method gives

$$R_{max}(n) = 47.7 + 5.29R_{min}(n) \pm 26.2 \qquad (14)$$

The correlation coefficient between these two parameters is $r = 0.723$ with a probability $P = 0.002$ that it is due to chance. This method, likewise, offers an improvement over using the mean cycle amplitude that is similar to that obtained using the Amplitude-Period Method. This relationship is shown in Figure 8.

3.2.2. Geomagnetic indicators. Geomagnetic indices have also been used to predict the amplitude of future cycles. *Ohl* [1966], for example, found that the minimum of the *aa* index is directly related to the

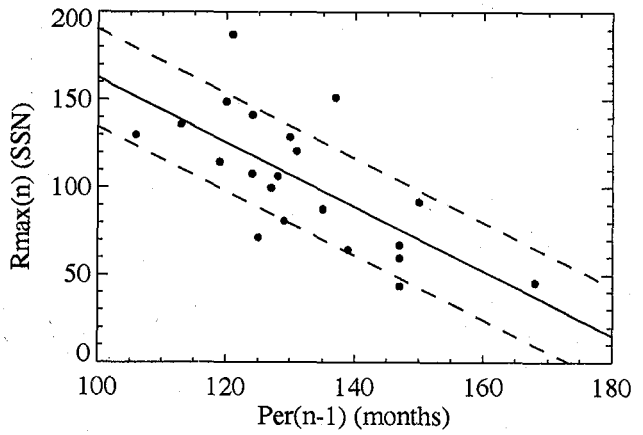

Figure 7. The Amplitude-Period Method for cycles 2-22. The maximum amplitude of a cycle is inversely proportional to the period of the preceding cycle. This relationship is shown with the solid line. The standard deviation about this line is shown with the dashed lines.

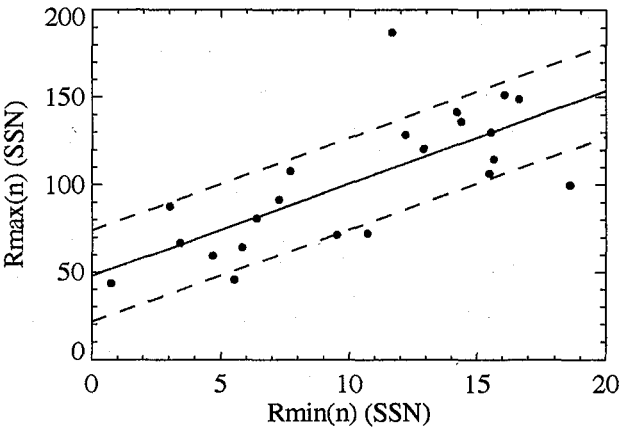

Figure 8. The Maximum-Minimum Method for cycles 1-22. The maximum amplitude of a cycle is proportional to the sunspot number at the minimum preceding it. This relationship is shown with the solid line. The standard deviation about this line is shown with the dashed lines.

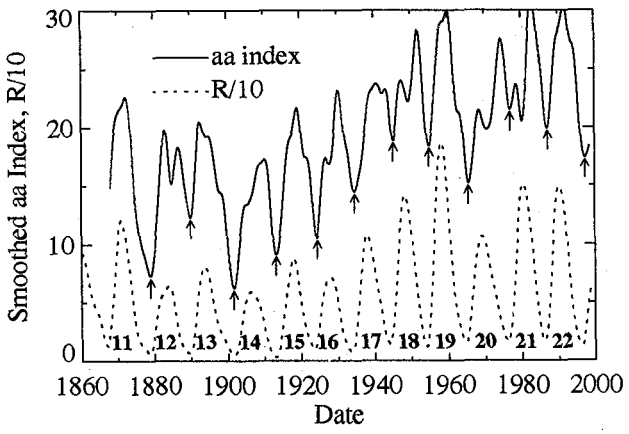

Figure 9. The smoothed *aa* index and sunspot numbers for cycles 11-22. The *aa* index at minima are identified with arrows. The heights of these minima appear to foreshadow the heights of the following sunspot maxima.

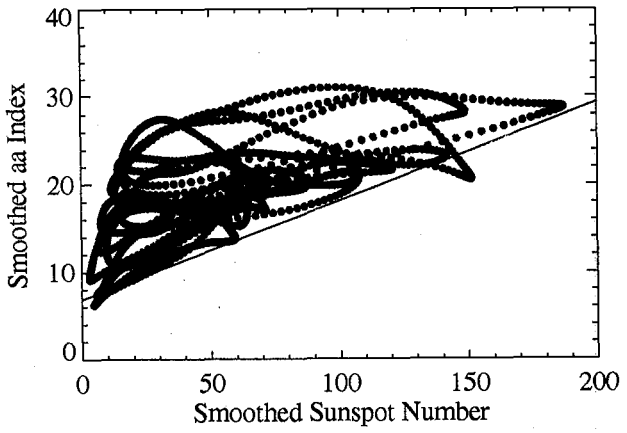

Figure 11. Our version of Feynman's Method for determining the dependence of the *aa* index upon the current sunspot number. A line is fit through the lowest values of the smoothed monthly *aa* index from each of 20 bins in smoothed monthly sunspot number.

maximum sunspot number for the following cycle. This method is similar to the Maximum-Minimum Method but uses the *aa* index at its minimum. The method is illustrated in Figure 9 using the 24-month Gaussian filtered *aa* index and International Sunspot Number. The minima of each cycle's *aa* index are identified with arrows.

The relationship between the minimum of the *aa* index and the maximum sunspot number for cycles 12-22, the cycles for which we have geomagnetic data, gives the Ohl's Method prediction with

$$R_{max}(n) = 8.9 + 7.20 aa_{min}(n) \pm 17.6 \qquad (15)$$

This relationship is shown in Figure 10. The two quantities are highly correlated with a correlation coefficient $r = 0.908$ and a probability $P = 0.002$ that this is due to chance. The standard deviation between the observed sunspot maxima and those obtained from this relationship is less than half that given using a mean cycle.

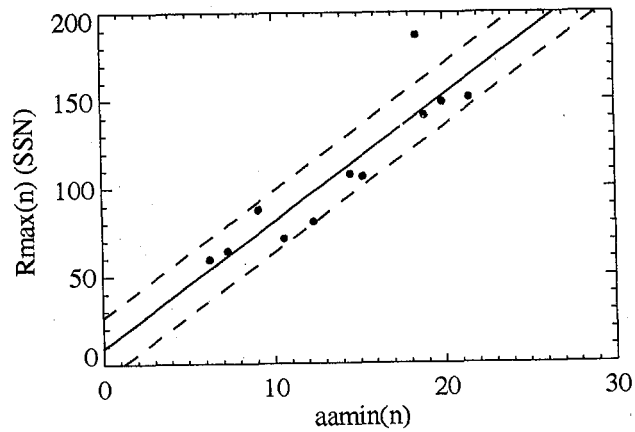

Figure 10. Ohl's Method for cycles 12-22. The maximum amplitude of a cycle is proportional to the *aa* index at the minimum preceding it. This relationship is shown with the solid line. The standard deviation about this line is shown with the dashed lines.

An alternative prediction method using the *aa* index was devised by *Feynman* [1982]. She noted that the *aa* index could be separated into two components - a component directly related to the current sunspot number and a second component she identified as an "interplanetary component." The sunspot number component is identified with the base level of the *aa* index as shown in Figure 11. As the sunspot number increases the *aa* index remains above some base level that increases linearly with sunspot number. Feynman used yearly averages of both aa and sunspot number and fit a line through the lowest points. This gives undue emphasis to the two lowermost points that define this line. Here we choose to alter the method by using the smoothed monthly values and binning the data into 20 bins according to the sunspot number (e.g. $R = [0-10, 10-20, \ldots 190-200]$) and then fitting a straight line through the lowest *aa* index values in those bins. This gives

$$aa_R(t) = 6.8 + 0.11 R(t), \qquad (16)$$

where the subscript R identifies this as the component that varies with the sunspot number. The relationship given by equation (16) is represented by the diagonal line in Figure 11.

The "interplanetary" component, aa_I, is constructed by subtracting the smoothed sunspot number component from the smoothed *aa* index. These two components are plotted as functions of time in Figure 12. Feynman noted that aa_I pre-shadowed the sunspot cycle. The size of the aa_I maxima are well correlated with the sunspot number maxima and occur several years prior to the sunspot maxima, in fact, they often occur well before sunspot minimum. The relationship

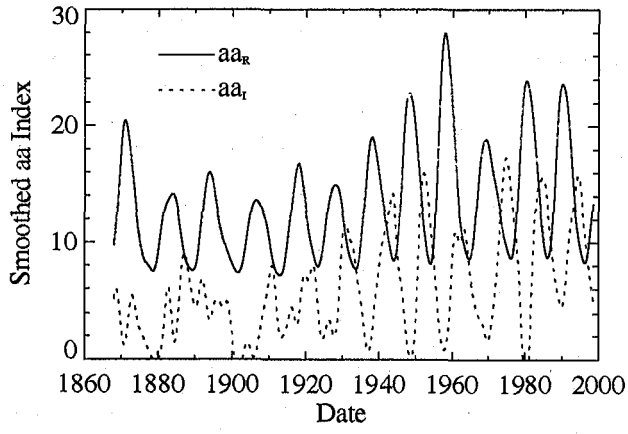

Figure 12. The two components of the *aa* index. The solid line represents the sunspot number component aa_R while the dotted line represents the interplanetary component aa_I. The interplanetary component mimics the sunspot number component but leads it in time by several years.

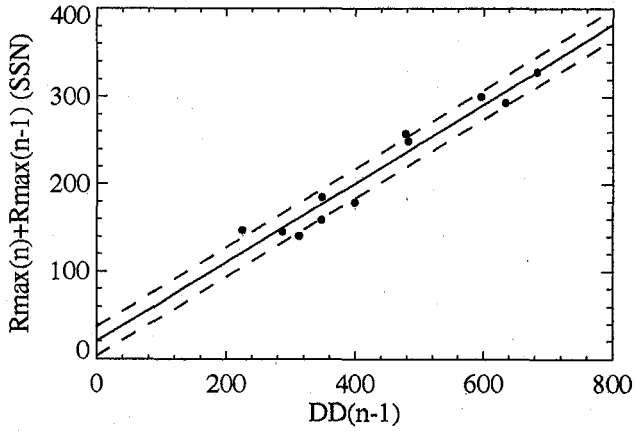

Figure 14. Thompson's Method for cycles 12-22. The maximum amplitude of a cycle is proportional to the number of geomagnetically disturbed days in the cycle preceding it. This relationship is shown with the solid line. The standard deviation about this line is shown with the dashed lines.

between these maxima in aa_I and R is shown in Figure 13. This relationship gives Feynman's Method for predicting the cycle amplitude as

$$R_{max}(n) = 7.8 + 9.26 aa_{Imax}(n) \pm 13.2 \qquad (17)$$

having a correlation coefficient $r = 0.950$ with a negligible probability that it is due to chance. The standard deviation for the sunspot maxima using this method is about one-third that given using the mean cycle amplitude.

A third method of sunspot cycle prediction using the geomagnetic indices is due to *Thompson* [1993]. He found that the number of geomagnetically disturbed days (defined as $Ap \geq 25$) that occurred during a sunspot cycle was proportional to the sum of the sunspot number amplitudes of that cycle and the following cycle. This is illustrated in Figure 14. The sum of the amplitudes for two consecutive cycles is plotted against the total number of geomagnetically disturbed days for the first of the cycle pairs. The relationship between these quantities gives Thompson's Method for predicting the cycle amplitude as

$$R_{max}(n) = 19.8 + 0.452 DD(n-1) - R_{max}(n-1) \pm 16.8, \qquad (18)$$

where $DD(n)$ is the number of geomagnetically disturbed days in cycle n. This relationship has a correlation coefficient $r = 0.971$ and a negligible probability that it is due to chance. (The *Ap* index itself is used from 1932 onward while the number of disturbed days for cycles 11-16 was determined from the *aa* index by Thompson.)

The quantities derived for use with these geomagnetic precursor methods are given in Table 2. The cycle num-

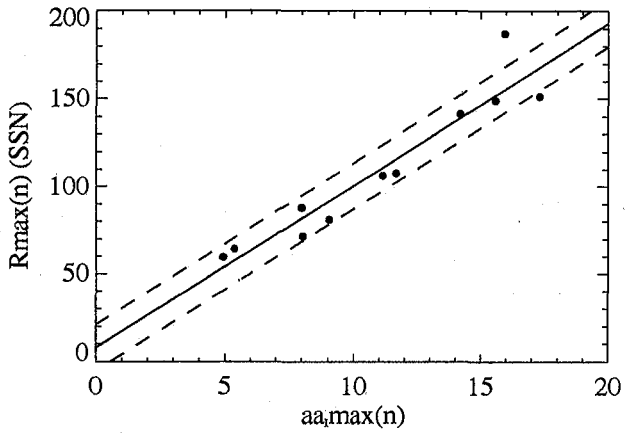

Figure 13. Feynman's Method for sunspot cycles 12-22. The maximum amplitude of a cycle is proportional to the maximum in aa_I near the minimum preceding it. This relationship is shown with the solid line. The standard deviation about this line is shown with the dashed lines.

Table 2. Geomagnetic Precursors Derived With the 24-Month FWHM Gaussian Filter

n	aa_{min}	*Date*	aa_{Imax}	*Date*	*DD*	R_{max}
11					348	120.7
12	7.3	1878/12	5.37	1873/02	287	64.3
13	12.3	1890/01	9.05	1887/03	313	81.0
14	6.2	1901/09	4.92	1898/08	225	59.5
15	9.1	1913/03	7.98	1910/10	348	87.8
16	10.6	1924/04	8.03	1921/12	399	71.5
17	14.5	1934/08	11.66	1930/11	482	107.9
18	18.9	1945/02	14.19	1943/07	683	141.5
19	18.4	1954/11	15.93	1952/04	634	187.2
20	15.2	1965/07	11.13	1963/06	478	106.5
21	21.5	1976/12	17.29	1974/08	596	151.4
22	19.9	1987/03	15.56	1984/10	624	149.0
23	17.5	1997/05	15.77	1994/06		

ber is given in the first column. The minimum in the *aa* index is given in the second column and the epoch of this minimum is given in the third column. The maximum in the "Interplanetary" component of the *aa* index and the epoch of its occurrence is given in the fourth and fifth columns. The number of disturbed days during the cycle is given in the sixth column and the final column gives the observed sunspot maximum.

The prediction techniques based on geomagnetic indices appear to be quite reliable as judged by the size of the standard deviations from the observed values and the strength of the correlations between the future maximum amplitude and the indices used. The method of *Ohl* [1966], however, has a disadvantage in the timing of its prediction. The years in which the minima in the *aa* index occur often coincide with sunspot minimum but can occur a year later. Since minimum is not identified until a rise is seen, this means that a prediction is not available until about a year or two following sunspot minimum. With the method of *Feynman* [1982], however, the maximum in the interplanetary component, aa_I, often occurs $\tilde{2}$ years before sunspot minimum and thus provides a prediction well in advance of that given using Ohl's method. The method of *Thompson* [1993] also gives an early prediction. Although it does not provide a final prediction until sunspot minimum is identified, it does give an estimate for the size of the next sunspot maximum that changes very little as sunspot minimum is approached and represents a lower limit. This is due to the fact that the number of disturbed days per month decreases dramatically near the time of sunspot minimum.

4. Testing Performance

The solar cycle prediction techniques described in the previous section can be tested using historical records of the sunspot cycle. For each technique we step backward in time and recalculate the relationships involved in the prediction technique using data from yet earlier times. This is done for cycles 19 through 22, which includes three large cycles and an average sized cycle (cycle 20). Testing with more cycles would obviously be advantageous but using earlier cycles decreases the number of cycles used in "calibrating" the prediction techniques.

The regression and curve-fitting techniques are tested at 6-month intervals starting 18 months after sunspot minimum. Predicted sunspot numbers for the remainder of the sunspot cycle are calculated at monthly intervals and compared to the observed (13-month running mean) values.

The precursor methods are tested at or near the time of sunspot minimum for each of the four test cycles. The relationships (equations (9)-(18)), involved in each of these techniques are redetermined using data from earlier times. These equations are then used to predict the size of the next cycle maximum and this prediction is compared to the observed value.

The results of testing the precursor methods are shown in Table 3. Columns 2-5 give the errors (predicted maximum - observed maximum) for each of the last four cycles. The last column gives the RMS of these errors for each of the prediction methods. This table shows that the geomagnetic precursor techniques (Ohl's Method, Feynman's Method, and Thompson's Method) give the most reliable predictions. Among these methods, Thompson's appears to be the best, but this is largely due to its accuracy in predicting the amplitude of cycle 19.

Table 3. Precursor Prediction Method Errors (Prediction - Observed) for Cycles 19-22

Prediction Method	19	20	21	22	RMS
Mean cycle	-94.8	-9.1	-53.5	-48.6	59.8
Secular trend	-91.6	8.7	-36.2	-25.3	51.0
Gleissberg cycle	-80.4	18.5	-51.6	-51.1	55.0
Even-odd	-59.3	-	-22.3	-	44.8
Amplitude-period	-74.1	0.3	-61.2	-25.3	49.7
Maximum-minimum	-83.9	21.6	-22.9	-15.0	45.4
Ohl's method	-55.4	19.1	21.8	4.4	31.3
Feynman's method	-42.8	9.6	26.9	3.6	25.8
Thompson's method	-17.8	8.7	-26.5	-13.6	17.9

In the process of testing these methods we also noted how stable the prediction methods were. For example, the relationship given by equation (10) for the Secular Trend Method changes quite dramatically from cycle to cycle. The parameters of the Gleissberg cycle in equation (11) also change in that the best fit for the cycle period increases monotonically from 7.5 cycles to 8.4 cycles from precycle 19 to the present. The Even-Odd Method also changes dramatically after cycle 19 is included in the statistics. The slope of the relationship between the odd cycle and the even cycle changes by a factor of 2 between the cycle 19 and cycle 21 predictions. The last five methods in Table 3 are considerably more stable than the first five. Most of the coefficients determined for these methods do not vary by more than 10% from one cycle to the next. Feynman's Method and Thompson's Method stand out as the most stable.

Three of the regression and curve-fitting techniques were tested: the *Hathaway et al.* [1994] cycle-shape function, the Modified McNish-Lincoln method, and the MSAFE method described in section 3.1. The mathematical function of *Stewart and Panofsky* [1938] was found to give very poor results for some cycles (cycles 1, 5, 7, 12, and 20). The function offered by *Elling and Schwentek* [1994] required more parameters with no improvement over the fit given with the function proposed by Hathaway et al. These three techniques were tested on each of the last four cycles at 6-month intervals. Each method was used to predict the remainder of the cycle at monthly intervals. The standard deviation of the difference between the predicted sunspot numbers and the 13-month running mean of the observed numbers was calculated for each prediction method at

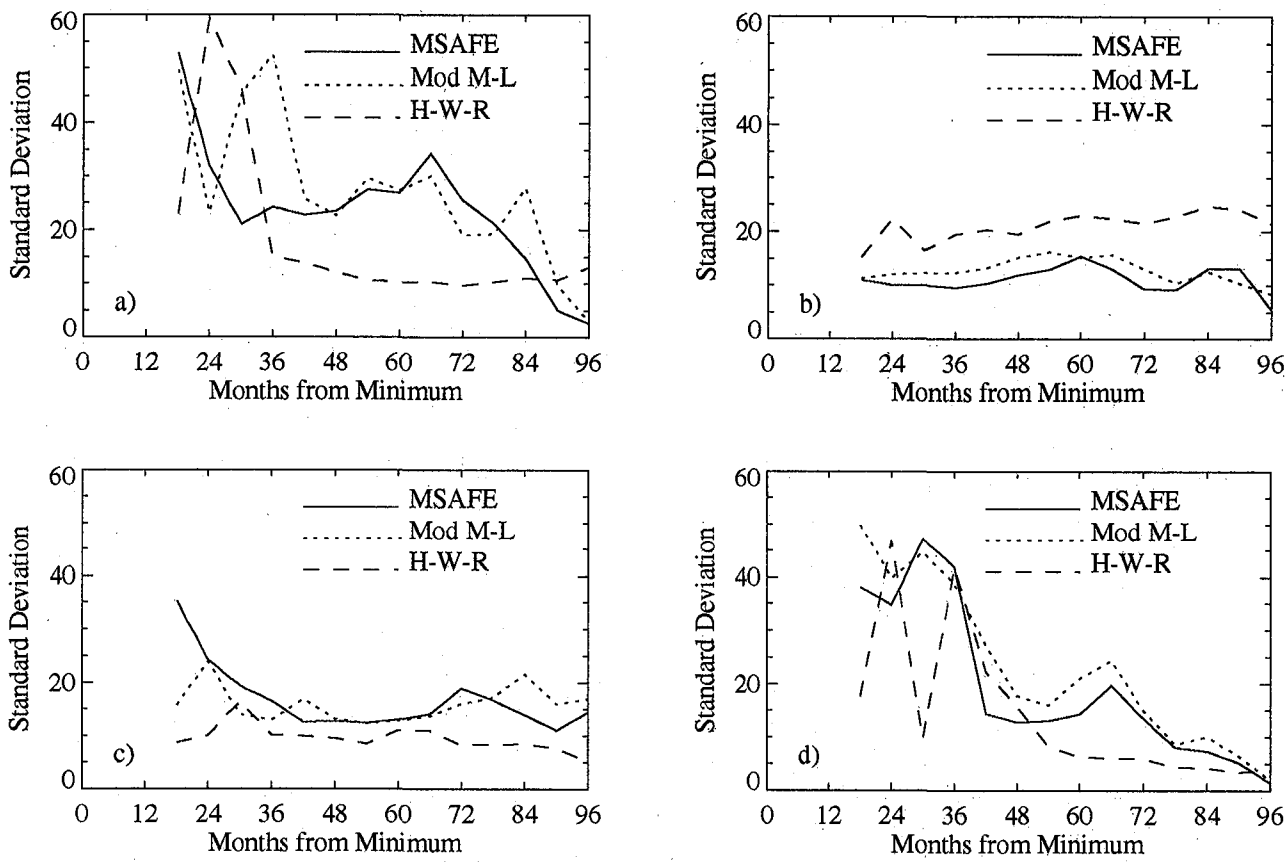

Figure 15. The standard deviation between the observed (13-month running mean) sunspot numbers and those predicted by the MSAFE, Modified McNish-Lincoln, and Hathaway-Wilson-Reichmann methods for cycles (a) 19, (b) 20, (c) 21, and (d) 22.

each point within these cycles. The Modified McNish-Lincoln Method and the MSAFE Method use the 13-month running of the sunspot number to predict future values (using unsmoothed monthly numbers is quite unstable with these methods). The best fit parameters for the function of Hathaway et al. were determined using the nonlinear least-squares fitting method of Marquardt and Levenberg as described by *Press et al.* [1986]. With this method the individual monthly averaged sunspot numbers are used.

The results of this testing of the regression techniques are shown in the four panels of Figure 15. The standard deviations between the predicted and observed (13-month running mean) sunspot numbers for the remainder of each cycle are plotted for the three methods (MSAFE, Modified McNish-Lincoln, and Hathaway-Wilson-Reichmann) as functions of the time since sunspot minimum. Cycle 19 is shown in Figure 15a, cycle 20 in Figure 15b, cycle 21 in Figure 15c, and cycle 22 in Figure 15d. In general, the deviations drop to lower levels near the time of sunspot maximum ($\tilde{4}8$ months from minimum). For three of the four cycles the curve-fitting of Hathaway et al. outperforms the MSAFE or Modified McNish-Lincoln Methods. For cycle 20, the average sized cycle, the MSAFE and Modified McNish-Lincoln methods performed better.

5. Synthesis: Improving Performance

A synthesis of these methods may yield an improved prediction method. An obvious choice is to use some combination of the precursor methods in order to predict cycle maximum and to use a cycle-shape formula for the month-by-month predictions. As the cycle progresses, the regression techniques ultimately become more accurate than the precursor techniques and the prediction technique should revert to these more accurate methods. We begin by finding a linear combination of precursor techniques that provides an improved early prediction of cycle maxima. We then determine how to transition from precursor estimates of the cycle to the cycle-shape fitting method as cycle maximum is approached.

It is apparent from the last section that some of the precursor techniques provide little improvement over using the mean cycle amplitude as a prediction for the next maximum. Three methods were found to be both ineffective and unstable. These include the Secular Trend, Gleissberg Cycle, and Even-Odd methods; so, for these reasons we drop them from further consideration. Some linear combination of the last five methods in Table 3 may provide an improved prediction. This will only be true, however, if they offer dif-

Table 4. Correlations between Precursor Method Errors (Prediction - Observed) for Cycles 12-22

	F	T	O	M	A
Feynman	-	0.08	0.96	0.50	0.35
Thompson	0.08	-	0.16	0.21	0.48
Ohl	0.96	0.16	-	0.67	0.47
Max-Min	0.50	0.21	0.67	-	0.57
Amp-Per	0.35	0.48	0.47	0.57	-

ferent predictions for each cycle. Ideally we would like to combine methods whose prediction errors are anticorrelated. The correlation coefficients between the prediction errors for these methods are given in Table 4 for cycles 12-22, the cycles for which geomagnetic indices are available.

Table 4 shows that all five methods are positively correlated. In particular, Feynman's Method and Ohl's Method are highly correlated ($r = 0.96$) so little would be gained from a combination of these two methods. On the other hand, Feynman's Method and Thompson's Method are uncorrelated ($r = 0.08$). A combination of these two methods should therefore give improved predictions. Using weights that are inversely proportional to the variance (standard deviation squared) of their prediction errors, we give a Combined Precursor Method with

$$R_{max}(n) = 12.4 + 5.72aa_{Imax}(n) + 0.173DD(n-1) - 0.382R_{max}(n-1) \pm 10.7, \quad (19)$$

which gives a smaller standard deviation for the prediction errors than either of the two parent methods (10.7 versus 16.8 and 13.2). We drop Ohl's Method from further consideration for three reasons: (1) its prediction errors are highly correlated with those from Feynman's Method, (2) its prediction errors are larger than those from Feynman's Method and, (3) its prediction is not available until much later in time than with Feynman's Method. Our attempts to incorporate the Maximum-Minimum Method and Amplitude-Period Method increased the standard deviation of the predictions due to the size of their errors (standard deviations of 26.2 and 28.7 respectively). Consequently, these two methods were also excluded from the Combined Precursor Method.

This Combined Precursor Method can be tested in the same manner as the other precursor methods by recalculating the method prior to each of cycles 19-22. We find that the method is stable in that the derived relationships and the calculated weights do not vary substantially from cycle to cycle. The prediction errors for cycles 19-22 are -38.4, 9.3, 5.3, and -3.2, respectively, with an RMS error of 20.0. Comparing these errors with those given in Table 3 shows that we attain a dramatic improvement in the predictions for cycles 21 and 22 and good performance for cycle 19 and 20. This method gives a predicted maximum of 154 ± 21 for cycle 23, where this error estimate represents the 95% confidence limits (twice the standard deviation).

The amplitude determined from the Combined Precursor Method can be used with either a rescaled mean cycle or the cycle-shape function of Hathaway et al. to predict the sunspot numbers over the next solar cycle. We prefer the cycle-shape function (equations (7) and (8)) because of its superior performance in three of the last four cycles and its ability to adjust its shape for changes associated with cycle amplitude.

A final synthesis of prediction techniques is achieved by using the Combined Precursor Method to determine the cycle amplitude at the start of the cycle and then switching over to using the fit to the cycle-shape function as the cycle progresses. As with the formulation of the Combined Precursor Method, this "Combined Solar Cycle Activity Forecast" uses weights that are inversely proportional to the variance (standard deviation squared) of the errors from each method. The weights are determined by computing the average of the standard deviations between the observed sunspot numbers and those predicted using either the Combined Precursor Method with the cycle-shape function or the fit to the cycle-shape function. These average deviations, along with those obtained with the Combined Solar Cycle Activity Forecast Method, are shown in Figure 16 for the last 11 cycles (the cycles for which the geomagnetic indices are available).

The weights determined from Figure 16 for this Combined Solar Cycle Activity Forecast Method are well-approximated by

$$W(t) = 1.0 - 0.6(1 - e^{-t^2/40^2}), \quad (20)$$

where this weight W is for the Combined Precursor Method and its complement, $1 - W$, is the weight of

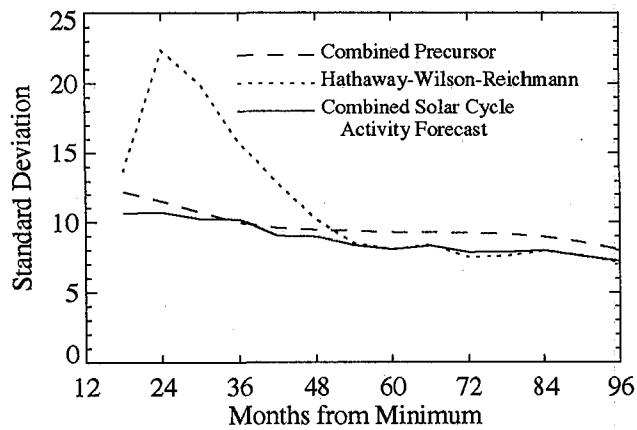

Figure 16. The standard deviation between the observed (24-month FWHM Gaussian filtered) sunspot numbers and those predicted by the Combined Precursor, the Hathaway- Wilson-Reichmann method, and the Combined Solar Cycle Activity Forecast Method. The Combined Solar Cycle Activity Forecast Method provides the best estimate of future sunspot numbers.

the Hathaway et al. Method. Time t is measured in months from minimum in equation (20). This can be used as early as 18 months into a cycle. The Combined Precursor Method alone should suffice prior to that time. It is somewhat surprising, in fact, how well the Combined Precursor Method alone does throughout the cycle.

The prediction for cycle 23 using this Combined Solar Cycle Activity Forecast Method in January 1999 is shown in Figure 17. The thick line in Figure 17 gives the predicted monthly values for the remainder of cycle 23. The dotted lines are placed at plus and minus two standard deviations as estimated from the solid line in Figure 16 at 30 months into the cycle. The Combined Precursor Method alone gives a cycle amplitude of 154 for cycle 23. When this prediction is combined with the fit to cycle 23 using the weights from equation (20) we find that the maximum falls slightly to 146.

6. Conclusions

In this study we have examined and tested several methods for the prediction of solar cycle variations in solar activity. We suggest that solar activity indices (sunspot number, 10.7-cm radio flux, etc.) should be filtered with the 24-month Gaussian-shaped filter to provide a better estimate of the solar activity variations on a solar cycle time scale. The traditional 13-month running means exhibit variations on timescales as short as 6 months and thus do not faithfully represent the solar cycle behavior. The short-term variations, with typical timescales from 27 days to 6 months to 2 years, are subjects of other studies and other prediction methods.

The solar cycle prediction methods were separated into two groups: precursor methods and regression methods. The precursor methods provide an estimate of the size of the maximum of the next cycle, while the regression methods provide a month-by-month estimate of the cycle's activity levels. We found that although several precursor methods were statistically significant, only two, Thompson's Method [*Thompson,* 1993] and Feynman's Method [*Feynman,* 1982], are needed to provide a better early estimate for the amplitude of the next cycle. Fortunately, the errors in the predictions by these two methods are uncorrelated so that an average of the two predictions as given by equation (19) is more accurate than either of the two alone. We found that the curve-fitting method of *Hathaway et al.* [1994] provides a reliable method for predicting the month-to-month variations in solar activity and that this method outperforms the Combined Precursor Method as the time of cycle maximum nears (Figure 16). The Combined Solar Cycle Activity Forecast Method uses a weighted average (equation (20)) of the Combined Precursor prediction and the Hathaway, Wilson, and Reichmann prediction to provide a better forecast of future solar cycle activity levels.

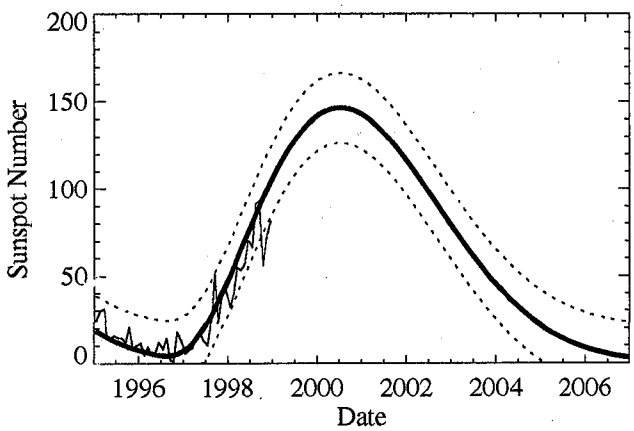

Figure 17. The prediction for cycle 23 obtained with the Combined Solar Cycle Activity Forecast Method. The thick line shows the predicted sunspot numbers. The dotted lines show the expected 5 and 95 percentile levels. The thin line shows the monthly averaged sunspot numbers through December 1998.

Our Combined Precursor Method alone is found to work especially well. In fact, it seems to work so well that the prediction provided by the Combined Solar Cycle Activity Forecast Method gives only a modest improvement. It should be noted that for cycle 23 NOAA now uses an amplitude prediction [*Joselyn et al.,* 1997] that is based largely on the geomagnetic precursors and then rescales the average-cycle shape to this maximum (160 ± 30) to predict the level of activity over the next cycle (J. Joselyn, private communication, 1998).

The varying success of these prediction methods suggests several interesting properties of the solar cycle. For example, although the Amplitude-Period Method and the Maximum-Minimum Method were both found to be less precise predictors of the next cycle's maximum amplitude, the fact that the relationships were statistically significant indicates that large-amplitude cycles start early and have high levels of activity at minimum. These relations suggest that the overlap of the cycles at the time of minimum is an important aspect of the solar cycle. The success of the precursor methods based on the geomagnetic indices, [*Ohl,* 1966; *Feynman,* 1982; *Thompson,* 1993] suggests a more substantial overlap between cycles. Thompson's Method uses the number of geomagnetically disturbed days throughout the entire previous cycle to predict cycle amplitudes well before the time of minimum. Likewise, Feynman's Method also provides a prediction for the amplitude of the cycle well before minimum. The surprising success of these precursor methods suggests that magnetic activity at latitudes above those populated by the sunspots of the current cycle may be the source of the solar wind disturbances that give rise to these precursor disturbances. This idea of an extended or two-component solar cycle [*Simon and Legrand,* 1992] needs further investigation.

The solar cycle prediction methods developed in the course of this study provide forecasts of future solar activity that are significantly better than those given by the mean cycle (equation (9)). These methods still

lack, however, a physical foundation based on dynamo theory. Efforts to invoke dynamo theory by including observations of the sun's polar magnetic field [*Schatten et al.*, 1978, *Schatten and Pesnell*, 1993, *Schatten et al.*, 1996] are noteworthy and promising but are based on only two solar cycles of magnetic data. Efforts were made by *Schatten et al.* [1978] to extend this data to earlier cycles using proxies for the polar magnetic field. However, these proxies were shown to be unreliable by *Layden et al.* [1991]. With reliable data for only the two most recent (and very similar) cycles, this technique could not be tested with any confidence. Such efforts are also somewhat premature in that a comprehensive and self-consistent dynamo model for the sun has not been produced. Development of a dynamo based prediction technique is, however, another key area for further investigation.

Finally, on the basis of our analysis presented here, we predict that cycle 23 will have a maximum amplitude near 150 (slightly higher if expressed as a 13-month running mean) with the maximum occurring midway through the year 2000. Activity for the next 3-4 years (1999-2002) should be typical of the maximum phase condition [cf. *Wilson et al.*, 1998b]. Although this prediction should not change much as the cycle progresses, we update the prediction every month as new data becomes available and post it on a world wide web site at http://science.nasa.gov/ssl/pad/solar/predict.htm.

Acknowledgments. This study was funded by the U.S. National Aeronautics and Space Administration through its Space Environment and Effects Program. None of this research would have been possible without the dedicated work by numerous solar observers over the last 390 years. We are particularly indebted to the current curators of those observations at the Sunspot Index Data Center in Brussels, Belgium, at the U.S. National Oceanic and Atmospheric Administration in Boulder, Colorado, at the National Solar Observatory in Tucson, Arizona, and at the Dominion Radio Astrophysical Observatory in Penticton, British Columbia. We also gratefully acknowledge several useful comments and suggestions on the manuscript by William W. Vaughan.

Janet G. Luhmann thanks both of the referees for their assistance in evaluating this paper.

References

Calvo, R. A., H. A. Ceccatto, and R. D. Piacentini, Neural network prediction of solar activity, *Astrophys. J., 444,* 916-921, 1995.

Conway, A. J., K. P. Macpherson, G. Blacklaw, and J. C. Brown, A neural network prediction of solar cycle 23, *J. Geophys. Res., 103,* 29,733-29,742, 1998.

Elling, W., and H. Schwentek, Fitting the sunspot cycles 10-21 by a modified F-distribution density function, *Sol. Phys., 137,* 155-165, 1992.

Feynman, J., Geomagnetic and solar wind cycles, 1900-1975, *J. Geophys. Res., 87,* 6153-6162, 1982.

Gleissberg, W., Probability laws of sunspot variations, *Astrophys. J., 96,* 234-238, 1942.

Gnevyshev, M. N., and A. I. Ohl, On the 22-year solar activity cycle, *Astron. Z., 25,* 18-20, 1948.

Greer, M. S., New procedures for SESC sunspot number and 10.7 cm flux prediction, in *Solar Terrestrial Predictions - IV: Proceedings of a Workshop at Ottawa, Canada,* vol. 2, edited by J. Hruska, M. A. Shea, D. F. Smart, and G. Heckman, pp. 172-179, National Oceanic and Atmospheric Administration, Environmental Research Laboratories, Boulder, Colo., 1993.

Hathaway, D. H., R. M. Wilson, and E. J. Reichmann, The shape of the solar cycle, *Sol. Phys., 151,* 177-190, 1994.

Holland, R. L., and W. W. Vaughan, Lagrangian least-squares prediction of solar flux (F10.7), *J. Geophys. Res., 89,* 11-16, 1984.

Joselyn, J., et al., Panel achieves consensus prediction of solar cycle 23, *Eos Trans. AGU, 78,* 205, 211-212, 1997.

Layden, A. C., P. A. Fox, J. M. Howard, A. Sarajedini, K. H. Schatten, and S. Sofia, Dynamo-based scheme for forecasting the magnitude of solar activity cycles, *Sol. Phys., 132,* 1-40, 1991.

Mayaud, P. N., *Derivation, Meaning, and Use of Geomagnetic Indices, Geophys. Monogr. Ser.* vol. 22, 154 pp., AGU, Washington, D. C., 1980.

McNish, A. G., and J. V. Lincoln, Prediction of sunspot numbers, *Eos Trans. AGU, 30,* 673-685, 1949.

Neihuss, K. O., H. C. Euler, Jr., and W. W. Vaughan, Statistical technique for intermediate and long-range estimation of 13-month smoothed solar flux and geomagnetic index, *NASA Tech. Memo., TM-4759,* 81 pp., 1996.

Ohl, A. I., Forecast of sunspot maximum number of cycle 20, *Solice Danie 9,* 84, 1966.

Press, W. H., B. P. Flannery, S. A. Teukolsky, and W. T. Vetterling, *Numerical Recipes: The Art of Scientific Computing,* Cambridge Univ. Press, New York, 1986.

Schatten, K. H., and W. D. Pesnell, An early solar dynamo prediction: Cycle 23 ~ Cycle 22, *Geophys. Res. Lett., 20,* 2275-2278, 1993.

Schatten, K. H., P. H. Scherrer, L. Svalgaard, and J. M. Wilcox, Using dynamo theory to predict the sunspot number during solar cycle 21, *Geophys. Res. Lett., 5,* 411-414, 1978.

Schatten, K., D. J. Myers, and S. Sofia, Solar activity forecast for solar cycle 23, *Geophys. Res. Lett., 23,* 605-608, 1996.

Simon, P. A. and J. P. Legrand, Toward a model of a two-component solar cycle, *Sol. Phys. 141,* 391-410, 1992.

Stewart, J. Q., and H. A. A. Panofsky, The mathematical characteristics of sunspot variations, *Astrophys. J., 88,* 385-407, 1938.

Thompson, R. J., A technique for predicting the amplitude of the solar cycle, *Sol. Phys., 148,* 383-388, 1993.

Vitinskii, Yu. I., Solar Activity Forecasting, *NASA TTF-289,* 129pp, NASA, Washington, D. C., 1965.

Waldmeier, M., Neue eigneschaften der sonnenfleckenkurve, *Astron. Mitt. Zurich, 14* (133), 105-130, 1935.

Waldmeier, M., Sunspot Activity, *Astron. Mitt. Zurich, 14* (138), 439, 470, 1939.

Wilson, R. M., An early estimate for the size of cycle 23, *Sol. Phys., 140,* 181-193, 1992.

Wilson, R. M., D. H. Hathaway, and E. J. Reichmann, An estimate for the size of cycle 23 based on near minimum conditions, *J. Geophys. Res., 103,* 6595-6603, 1998a.

Wilson, R. M., D. H. Hathaway, and E. J. Reichmann, Estimating the size and timing for cycle 23 from its early cycle behavior, *J. Geophys. Res., 103,* 17,411-17,419, 1998b.

Wolf, R., Bestimmung der epochen fur das minimum und maximum der sonnenflecken-bildung, *Naturf. Gesell. Bern Mitt.* 1852.

D. H. Hathaway, R. M. Wilson, and E. J. Reichmann, Mail Code SD50, NASA Marshall Space Flight Center, Huntsville, AL 35812. (david.hathaway@msfc.nasa.gov; robert.wilson@msfc.nasa.gov; ed.reichmann@msfc.nasa.gov)

(Received March 5, 1999; revised May 28, 1999; accepted July 13, 1999.)